

Electrophysiological Properties of Avian Basal Ganglia Neurons Recorded In Vitro

MICHAEL A. FARRIES AND DAVID J. PERKEL

Department of Neuroscience, University of Pennsylvania, Philadelphia, Pennsylvania 19104

Received 28 April 2000; accepted in final form 28 July 2000

Farries, Michael A. and David J. Perkel. Electrophysiological properties of avian basal ganglia neurons recorded in vitro. *J Neurophysiol* 84: 2502–2513, 2000. The forebrains of mammals and birds appear quite different in their gross morphology, making it difficult to identify homologies between them and to assess how far they have diverged in organization. Nevertheless one set of forebrain structures, the basal ganglia, has been successfully compared in mammals and birds. Anatomical, histochemical, and molecular data have identified the avian homologues of the mammalian basal ganglia and indicate that they are very similar in organization, suggesting that they perform similar functions in the two classes. However, the physiological properties of the avian basal ganglia have not been studied, and these properties are critical for inferring functional similarity. We have used a zebra finch brain slice preparation to characterize the intrinsic physiological properties of neurons in the avian basal ganglia, particularly in the input structure of the basal ganglia, the striatum. We found that avian striatum contains a cell type that closely resembles the medium spiny neuron, the principal cell type of mammalian striatum. Avian striatum also contains a rare cell type that is very similar to an interneuron class found in mammalian striatum, the low-threshold spike cell. On the other hand, we found an aspiny, fast-firing cell type in avian striatum that is distinct from all known classes of mammalian striatal neuron. These neurons usually fired spontaneously at 10 Hz or more and were capable of sustained firing at very high rates when injected with depolarizing current. The existence of this cell type represents an important difference between avian striatum and mammalian dorsal striatum. Our data support the general idea that the organization and functional properties of the basal ganglia have been largely conserved in mammals and birds, but they imply that avian striatum is not identical to mammalian dorsal striatum.

INTRODUCTION

At first glance, the mammalian telencephalon bears little resemblance to the telencephalon of birds and other tetrapods. The mammalian telencephalon consists of a laminar cerebral cortex overlying masses of gray matter collectively known as the basal ganglia, while the forebrains of other tetrapods show few signs of this laminar organization. Indeed, the prevalent view before the 1960s was that little or nothing in the avian brain is homologous to the mammalian isocortex and held that most of the avian telencephalon consists of striatum, the largest component of the basal ganglia (reviewed in Striedter 1997).

Present address and address for reprint requests: D. J. Perkel, Depts. of Zoology and Otolaryngology, University of Washington, 1959 NE Pacific St. HSB BB1165, Box 356515, Seattle, WA 98195-6515 (E-mail: perkel@u.washington.edu).

Thus, the organization of the mammalian telencephalon seemed to differ radically from that of the avian telencephalon.

We now know that the brains of birds and mammals are much more alike than was originally believed. Only a small part of the avian brain, known as the “paleostriatal complex,” is actually a homologue of the mammalian basal ganglia (Karten and Dubbeldam 1973; Medina and Reiner 1995). The other parts of the avian telencephalon (called neostriatum, archistriatum, and hyperstriatum) are homologues of mammalian pallium, i.e., the cerebral cortex, claustrum, and pallial amygdala (Karten 1991; Puelles et al. 1999; Striedter 1997). The exact homologies between the various parts of the mammalian pallium and structures of the avian brain are still unclear (Striedter 1997), but comparison of the basal ganglia of the two classes seems comparatively straightforward. The main components of the basal ganglia in mammals are the striatum, which receives input from the cerebral cortex, and the globus pallidus, which receives GABAergic input from the striatum and sends GABAergic projections to the midbrain and thalamus. From anatomical (Karten and Dubbeldam 1973; Kitt and Brauth 1982; Medina and Reiner 1997; Veenman et al. 1995), histochemical (Medina and Reiner 1995), and molecular (Puelles et al. 1999; Smith-Fernandez et al. 1998) evidence we know that the avian homologues of the mammalian striatum are the paleostriatum augmentatum (PA) and the lobus parolfactorius (LPO), and the avian homologue of the globus pallidus is the paleostriatum primitivum (PP; see Fig. 1). The organization, projections, and neurochemical properties of the basal ganglia seem to be conserved between mammals and birds to a remarkable degree. This suggests that the basal ganglia of birds perform functions similar to those of the mammalian basal ganglia, using similar mechanisms.

However, anatomical and neurochemical organization do not fully determine how a neural structure works. Equally important are the intrinsic physiological properties of its neurons. Neurons in the basal ganglia of mammals have a characteristic set of physiological properties that have been well studied, particularly in the striatum (Jiang and North 1991; Kawaguchi 1993; Kita et al. 1984; Nisenbaum and Wilson 1995). Although the anatomical organization of the basal ganglia of birds and mammals has been largely conserved, their functions may still have diverged substantially through divergence in the physiological properties of their neurons. The goal

The costs of publication of this article were defrayed in part by the payment of page charges. The article must therefore be hereby marked “advertisement” in accordance with 18 U.S.C. Section 1734 solely to indicate this fact.

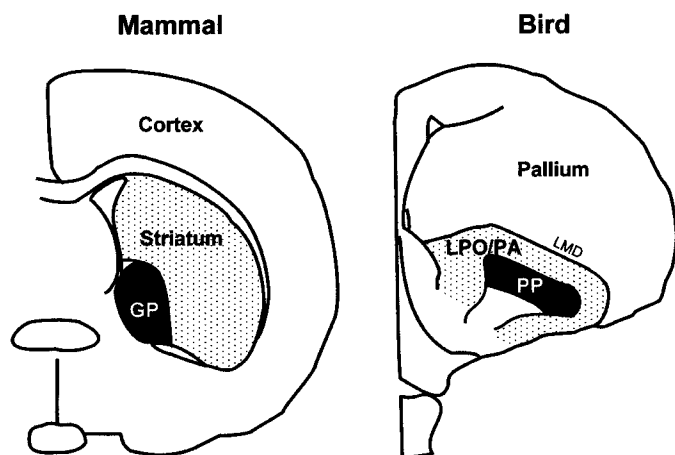


FIG. 1. Schematic coronal sections through the forebrains of mammals and birds. The stippled regions indicate striatum and the black regions are pallidum. GP, globus pallidus; LPO, lobus parolfactorius; PA, paleostriatum augmentatum; PP, paleostriatum primitivum; LMD, lamina medullaris dorsalis (the band of fibers that marks the boundary between the paleostriatal complex and the overlying pallium).

of this study is to examine the intrinsic physiological properties of neurons in the avian basal ganglia and assess their similarity to neurons of the mammalian basal ganglia. To address this issue, we have recorded from neurons in the zebra finch basal ganglia in a brain slice preparation, using the whole cell technique in current-clamp mode.

METHODS

Preparation of brain slices

Adult zebra finches were obtained from a local supplier; this study also employed juvenile zebra finches (31–71 days old) that were bred in our colony. Adult zebra finches were housed three to five per cage, while juvenile zebra finches were housed in cages containing only their parents and siblings. Birds were kept on a 13:11 h light:dark cycle. Slices were prepared as described by Stark and Perkel (1999), except for the composition of the artificial cerebrospinal fluid (ACSF) used during slicing (see following text). The procedures were approved by the Institutional Animal Care and Use Committee at the University of Pennsylvania. Briefly, birds were anesthetized with isoflurane and killed by decapitation. The brain was rapidly removed and placed in ice-cold ACSF containing (in mM) 119 NaCl, 2.5 KCl, 1.3 MgSO₄, 2.5 CaCl₂, 1 NaH₂PO₄, 16.2 NaHCO₃, 11 D-glucose, and 10 HEPES. Parasagittal or coronal brain slices, 300 μ m thick, were cut with a vibrating microtome and collected in ACSF heated to 30°C and subsequently allowed to cool to room temperature. The ACSF used for collecting slices and recording differed slightly from the ACSF used during slicing—the ACSF used for collecting and recording had 26.2 mM NaHCO₃ and no HEPES, but was otherwise identical to the ACSF used for slicing. All solutions were bubbled with a 95% O₂-5% CO₂ mixture.

Identification of PA, PP, and LPO in living brain slices

A thin layer of fibers, the lamina medullaris dorsalis (LMD; see Fig. 1), marks the boundary between the paleostriatal complex and the overlying neostriatum. PA and LPO lie immediately ventral to the LMD, which is clearly visible in living, unstained brain slices. The approximate boundary between PA and LPO in coronal slices lies at a “kink” in the LMD, where it turns more ventrally as one moves from lateral to medial portions of the slice. Recordings targeting PA were

made substantially lateral to this boundary; LPO recordings were made substantially medial to it. In parasagittal slices, no border could be seen between PA and LPO, and thus some cells recorded in these slices could not be definitively localized to PA or LPO. Accordingly, these cells are excluded from analyses comparing PA and LPO. The LPO of zebra finches contains a specialized region known as “area X,” found only in songbirds; cells in this area are not included in this study and will be described elsewhere. PP was identified as a densely fibrous region ventromedial to PA. Kuenzel and Masson (1988, pp. 10, 59, and 62) illustrate how PP can be identified in unstained coronal slices. In practice, however, we found that this fibrous region marks only the approximate location of PP in living slices; when the location of recorded neurons was confirmed with Nissl staining, many cells recorded while targeting PP proved to be in PA. Nevertheless cells recorded while targeting PA or LPO were always found in the targeted structure.

Electrophysiological recording

During experiments, slices were placed in a recording chamber and superfused with ACSF heated to 25–27°C. We recorded from neurons using the “blind” whole cell method (Blanton et al. 1989). Pipettes had a resistance of 5–9 M Ω and were filled with a solution containing (in mM) 120 K methylsulfate, 10 HEPES, 2 EGTA, 8 NaCl, and 2 Mg ATP, pH 7.2–7.4, osmolality 275–285 mOsm. In most cases, 0.5% neurobiotin (Vector Laboratories, Burlingame, CA) was included in the pipette solution to permit visualization of the recorded neuron. Signals were amplified using an Axoclamp 2B (Axon Instruments, Foster City, CA) followed by a Brownlee Model 410 amplifier (Brownlee Precision, Santa Clara, CA). Signals were low-pass filtered at 1–3 kHz, digitized at twice (or more) the filter cutoff frequency with a National Instruments (Austin, TX) digitizing board, and acquired using a custom data-acquisition program written in LabVIEW (National Instruments). Membrane potentials were corrected for a liquid junction potential of +5 mV. The only drug used in this study, 4-aminopyridine (4-AP), was obtained from Research Biochemicals (Natick, MA) and was bath-applied.

Histological procedures and morphological measurements

After recordings using neurobiotin in the pipette solution, slices were immersion-fixed in paraformaldehyde (4% in 0.1 M phosphate buffer) and kept at 4°C for at least 4 h. Slices were then transferred to a cold sucrose solution (30% in 0.1 M phosphate buffer) and stored at 4°C for several hours to several days. Slices were resectioned to 60 μ m thickness with a freezing microtome and processed for visualization with an avidin/biotin/horseradish peroxidase complex (ABC Elite Kit, Vector Laboratories) followed by a reaction using the Vector VIP peroxidase substrate kit (Vector Laboratories). In most cases in which the slices were counterstained with cresyl violet (Nissl stain), diaminobenzidine was used as the peroxidase substrate instead of the VIP kit since the VIP kit produces a purple precipitate that may be obscured in a Nissl-stained background. Labeled neurons were examined with a $\times 40$ objective ($\times 100$ in some cases), soma diameters along major and minor axes were measured, and the number of primary dendrites was counted. Cell diameters given in the text are averages of the major and minor axis diameters.

Analysis and measurement of electrophysiological parameters

We analyzed our recordings to measure basic electrophysiological parameters such as input resistance, action potential threshold, etc. We encountered difficulty in defining the input resistance for many neurons because the membrane resistance depended strongly on their membrane potential (the same problem occurs in mammalian striatal neurons, see Nisenbaum and Wilson 1995). Since different neurons of

the same class had different resting membrane potentials, they could exhibit dramatically different input resistances as calculated from their response to a small current pulse from rest. Such neurons might have exactly the same current-voltage relationship when brought to the same baseline membrane potential yet display very different input resistances simply because they happened to be resting at different potentials. To circumvent this problem, we define a cell's input resistance as the maximum slope of its current-voltage (I - V) curve at membrane potentials below -50 mV. We exclude the portion of the I - V curve more depolarized than -50 mV to minimize artifacts produced by depolarization-activated depolarizing currents such as those carried by Na^+ and Ca^{2+} . The I - V curve is generated from the steady-state voltage deflection produced by current pulses of 500- to 1,000-ms duration. Note that this excludes from the I - V curve the "ramping responses" many of our neurons produced when injected with depolarizing current pulses of sufficient magnitude (see Fig. 2A for an example). Voltage traces shown in figures are typically averages of two to six traces evoked by the same current pulse, except for traces containing action potentials.

We measured various aspects of action potentials using custom software written in IGOR (WaveMetrics, Lake Oswego, OR). The beginning of an action potential (AP) is defined as the averaged times of the maxima of the waveform's second and third derivatives. This definition was chosen because it provided the best match with our visual judgement of where the AP begins. The AP threshold is defined as the membrane voltage at this initiation point; the AP amplitude is the voltage at the peak minus the threshold voltage; the AP duration is its width at half height, the afterhyperpolarization (AHP) peak is the voltage minimum attained after the AP peak but before a point set by the user; the AHP time to peak is the time of this minimum minus the time when the membrane potential crosses the AP threshold on descent from the AP peak. For each cell, the measurements of five APs (where possible) were averaged to produce the final AP measurements for that cell. Only the first AP fired during a current pulse was used in these averages unless more APs were needed to achieve the standard five APs per cell. We also measured the "delay to first spike," defined as the time from the onset of a 500-ms depolarizing current pulse to the occurrence of the first AP in traces where only one AP was fired (if no such traces were available in a recording, we made this measurement on traces with the fewest APs).

RESULTS

Intrinsic electrophysiological properties of the principal cell type of PA and LPO

The most common neuronal type we recorded in PA and LPO ($n = 31$ cells, recorded from 14 birds) had a resting potential of 74 ± 11 (SD) mV and an input resistance of 383 ± 203 M Ω . We recovered 20 neurons of this type filled with neurobiotin and found that they have irregularly shaped somata (9.3 ± 1.8 μm diam) with four to seven primary dendrites. The dendrites were covered with spines (Fig. 2C), and so we designate these cells as "spiny neurons" (SNs). Spontaneous postsynaptic potentials were sometimes observed, but these cells never fired spontaneous action potentials when healthy. When these cells were injected with pulses of hyperpolarizing current, all exhibited time-independent inward rectification, i.e., a rapid decrease in membrane resistance (Fig. 2, A and B). A few SNs also displayed a small time-dependent component of this hyperpolarization-activated inward rectification ($n = 3$, data not shown). We quantified this inward rectification as the ratio of the minimum membrane resistance occurring on hyperpolarization to the input resistance as defined in METHODS. Among the SNs for which this measurement could be made ($n = 26$), the ratio was 0.35 ± 0.23 .

When injected with depolarizing current pulses, all SNs responded with a gradual, ramp-like increase in membrane potential (Fig. 2A). With a sufficiently strong or long-duration depolarizing current pulse, the ramping response ended with action potentials that were substantially delayed relative to the onset of the pulse (Figs. 2A and 3). We quantified this delayed spiking by measuring the time from the onset of a 500-ms depolarizing current pulse to the occurrence of the first spike, in traces where only one spike was fired (or, if no such traces were available, in traces where the smallest number of spikes were fired in that recording). The delay to first spike in SNs was 378 ± 70 ms; this measurement for other cell types is given in Table 1. After firing the first spike, these cells usually

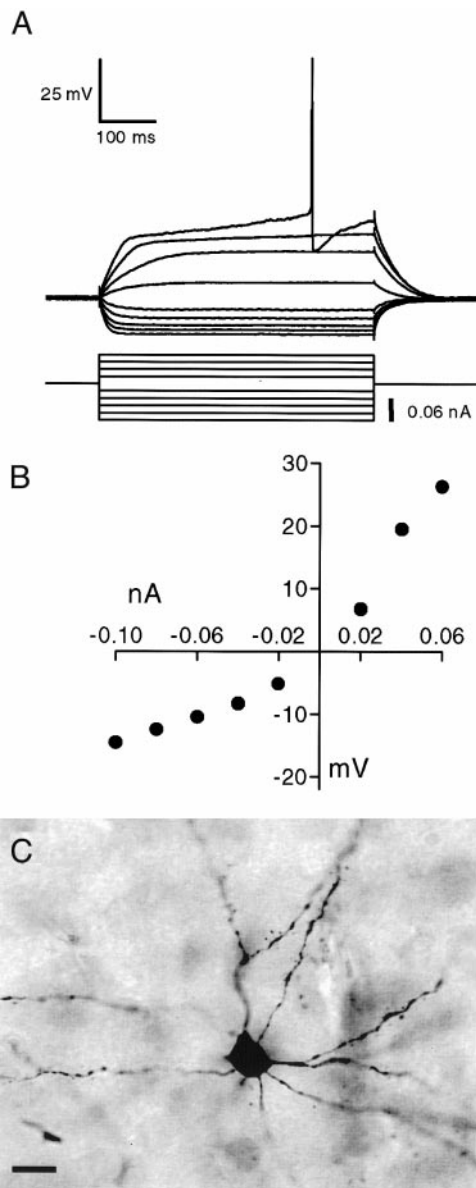


FIG. 2. Intrinsic properties of an avian striatal spiny neuron (SN), recorded in LPO. A: responses of this SN to a series of 500-ms current pulses delivered from rest (-78 mV). The size of these current pulses is plotted immediately below the voltage traces. B: graph of the steady-state voltage deflections from rest produced in this neuron as a function of the amplitude of the injected current pulse. C: photomicrograph of this SN filled with neurobiotin. Scale bar is 10 μm .

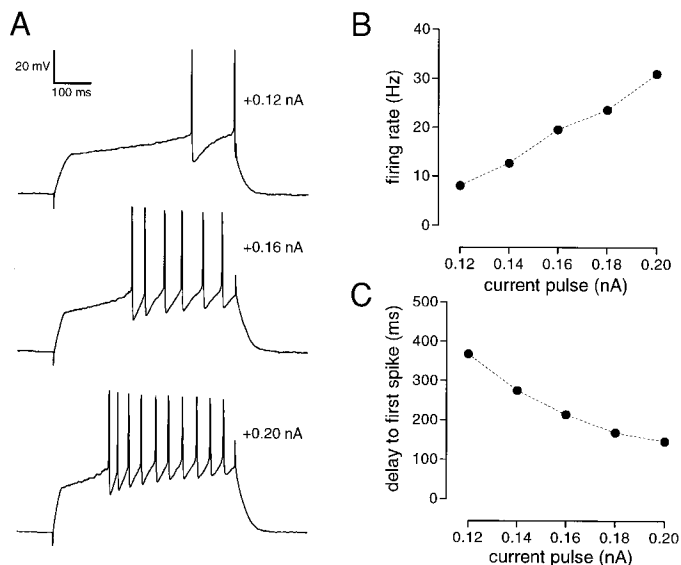


FIG. 3. Firing properties of SNs. *A*: response of a SN to 3 successively larger 500-ms current pulses. The amplitude of the current pulse is indicated next to each voltage trace. *B*: action potential frequency evoked in this SN as a function of the amplitude of the current pulse. This firing rate is defined as the inverse of the average interspike interval following the first spike, i.e., it excludes the “delay period” preceding the 1st spike. *C*: the delay from the onset of the current pulse to the occurrence of the 1st action potential as a function of the amplitude of the current pulse. Points in *B* and *C* are averages of the response to 2 repetitions of each current pulse.

fire repetitively, occasionally with some accommodation in firing rate (Fig. 3*A*). As stronger depolarizing pulses were injected, these cells fired action potentials at higher rates (Fig. 3*B*) with a shorter delay from onset of the pulse to the first spike (Fig. 3*C*). Additional electrophysiological parameters of SNs and other avian cell types are summarized in Table 1.

In the properties described above, these cells show no qualitative differences from the principal cell type of mammalian striatum, the medium spiny neuron (MSN). In particular, they share two defining properties: fast inward rectification in response to hyperpolarizing current and a ramping response to depolarizing current (Nisenbaum and Wilson 1995). In mammalian MSNs, the ramping response is mediated by an A-type K^+ current that rapidly activates on depolarization and then gradually inactivates, allowing a slow membrane depolarization. This current is blocked by 4-AP, and in mammalian MSNs 4-AP eliminates both the ramping response and the

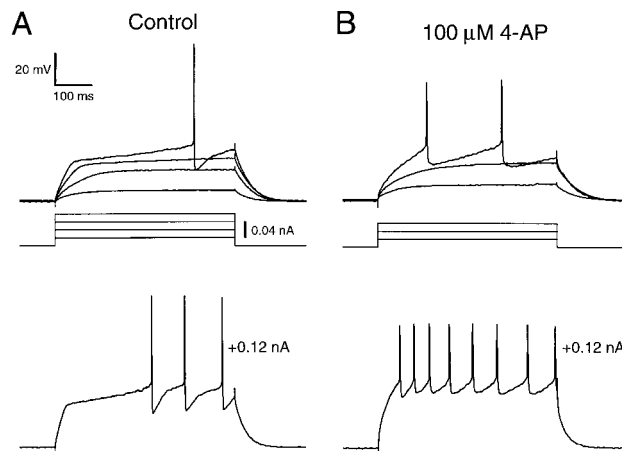


FIG. 4. Blockade of SN ramping response and delayed spiking by 4-aminopyridine (4-AP). *A*: response of a SN to depolarizing current pulses under control conditions. The amplitude of the current pulses is plotted under the traces (top 4 superimposed traces) or is indicated next to the voltage trace (bottom trace). *B*: response of the same SN to depolarizing current pulses after bath application of 100 μ M 4-AP. Scale is the same as in *A*. During prolonged whole cell recordings, the amplitude of action potentials in the recorded cell often decreased, in conjunction with an increase in the series resistance. This phenomenon is visible in the traces shown in *B*; it is not an effect of 4-AP. This cell is the one shown in Fig. 2.

delay in spiking (Nisenbaum and Wilson 1995; Nisenbaum et al. 1994). To further explore the mechanistic similarities between mammalian and avian spiny neurons, we examined the effect of 4-AP on avian striatal SNs. Bath application of 100 μ M 4-AP blocked the ramping response and the delayed spiking in these cells (Fig. 4, $n = 6/6$ cells from 4 birds; delay to first spike went from 449 ± 47 to 221 ± 76 ms on application of 4-AP, a statistically significant difference, paired Wilcoxon test, $P = 0.03$). This suggests that an A-type current is responsible for the ramping response and delayed spiking seen in avian striatal SNs, as it is in mammals.

Lack of age-related changes in the properties of spiny neurons in PA and LPO

Neurons in some regions of the zebra finch brain undergo changes in their physiological properties as the birds mature (Boettiger and Doupe 1998; Bottjer et al. 1998; Livingston and Mooney 1997; Stark and Perkel 1999; White et al. 1999). To examine the possibility of age-related changes in PA and LPO,

TABLE 1. Properties of avian striatal neurons

	SN	ASN	AF	LTS
Resting potential, mV	-74 ± 11	-72 ± 12^a	NA	-50 ± 7^b
Input resistance, $M\Omega$	383 ± 203^c	436 ± 181^d	414 ± 215	388 ± 243
AP threshold, mV	-34.5 ± 6.3	-42.7 ± 9.7	-44.9 ± 5.9	-43.3 ± 5.5
AP amplitude, mV	42.4 ± 10.3	51.0 ± 12.3	49.4 ± 12.7	46.8 ± 13.6
AP duration, ms	1.30 ± 0.28	1.66 ± 0.72	1.15 ± 0.55	1.84 ± 0.54
AHP peak, mV	-18.5 ± 4.0	-12.1 ± 5.6	-14.2 ± 6.9	-12.2 ± 2.9
AHP time to peak, ms	3.24 ± 2.17	2.50 ± 2.54	10.26 ± 9.80	2.83 ± 1.34
Delay to first spike, ms	378 ± 70	58 ± 58^e	147 ± 101	96 ± 58

Values in this table are means \pm SD. The resting potential for AF cells is listed as “NA” (not applicable) because they fired action potentials spontaneously. See METHODS for definitions of the various parameters presented here. The number of cells for SN, ASN, AF, and LTS are 31 cells from 14 birds, 21 cells from 16 birds, 9 cells from 8 birds, and 4 cells from 4 birds. SN, spiny neuron; ASN, anomalous spiny neuron; AF, aspiny, fast-firing neuron; LTS, low threshold spike neuron. In some cases, the data needed to measure all parameters for all cells were not available. In such cases, the number of cells contributing to the measurement is indicated in the following footnotes: ^a $n = 20$; ^b $n = 3$; ^c $n = 30$; ^d $n = 18$; and ^e $n = 20$.

we divided the cells into two major age groups—a juvenile group recorded from birds aged 31–46 days old (5 birds) and an adult group from birds at least 80 days old (8 birds). We compared SNs recorded in the two age groups, the only cell type common enough to permit comparison ($n = 10$ juvenile SNs, $n = 16$ adult SNs; 5 SNs recorded from a 72-day-old bird were excluded from this comparison). There were no qualitative differences between the two groups (e.g., both exhibited fast inward rectification, ramping depolarization, and delayed spiking) nor were there any significant differences in major electrophysiological properties (comparisons summarized in Table 2). For this reason, the data from these two age groups are combined in all other analyses.

Properties of a striatal interneuron cell type recorded in PA and LPO

Some of the neurons we recorded were not of the spiny neuron type, differing in physiological properties or morphology. Four of these neurons exhibited unusual firing properties resembling a mammalian striatal interneuron type, the “low-threshold spike” cell [LTS, also known as “PLTS” (Kawaguchi 1993), recorded from 4 birds]. Three of these neurons rested at relatively depolarized potentials (-50 ± 7 mV); the fourth fired spontaneously roughly once every 5 s. We examined the current-voltage relationship of these neurons by hyperpolarizing them to approximately -80 mV and delivering current pulses from that potential. These cells had an input resistance of 388 ± 243 M Ω . When injected with hyperpolarizing current pulses, these neurons exhibited time-dependent inward rectification to varying degrees, exemplified by a “sag” in the membrane potential near the onset of the current pulse (Fig. 5A). Depolarizing current pulses elicited a plateau-like spike lasting hundreds of milliseconds, typically crowned by one to three fast action potentials appearing at the beginning of the plateau-like potential (Fig. 5, A and B). This persistent spike was the defining characteristic of these neurons and was triggered at a membrane potential of -58 ± 2 mV. This spike (and the accompanying fast action potentials) could also be triggered on rebound following a hyperpolarizing current pulse (Fig. 5A). We recovered only one of these neurons filled with neurobiotin; this cell had aspiny dendrites, unlike the SN cell type (Fig. 5C).

Intrinsic electrophysiological properties of “anomalous” spiny neurons in PA and LPO

Another group of cells that differed from the SN type were morphologically indistinguishable from SNs (Fig. 6D shows an example) but possessed somewhat different physiological properties. These neurons, like SNs, displayed fast inward rectification in response to hyperpolarizing current pulses (minimum resistance:input resistance ratio of 0.18 ± 0.07 , $n = 15$) and produced a ramping response to depolarizing current pulses but were distinguished from ordinary SNs by their tendency to fire an action potential at the onset of suprathreshold current pulses (Fig. 6A). When injected with larger depolarizing current pulses, such cells either failed to fire more action potentials or fired additional action potentials that were unusually broad and of smaller amplitude. We recorded a total of 15 of these cells (from 11 birds); of these, 7 exhibited the firing properties of “normal” SNs during some part of the recording (i.e., at some point in the recording, they switched from the “normal” state to the “anomalous” state, or vice versa). Such behavior has been recorded in mammalian medium spiny neurons after intracellular dialysis (C. Wilson, personal communication).

A second population of “anomalous” spiny neurons ($n = 9$ cells from 8 birds) possessed fast inward rectification (minimum resistance:input resistance ratio of 0.41 ± 0.13) but showed no signs of a ramping response to depolarizing current pulses (Fig. 6B). These cells were generally capable of firing multiple action potentials during strong depolarizing current pulses that were not markedly different from healthy Na⁺ action potentials (6 of 8, Fig. 6C). In addition, these cells produced a small “bump” in membrane potential near the beginning of sufficiently strong depolarizing current pulses (Fig. 6B). In one case, a neuron with these properties switched to a “normal” SN state, i.e., began showing a ramping response to depolarizing current pulses and fired action potentials delayed relative to the onset of the current pulse (Fig. 6E).

Properties of an aspiny, fast-firing cell type in PA and LPO

We identified one other cell type in avian striatum that was distinct from the SN class and yet did not closely resemble any of the striatal interneuron types found in mammals (Fig. 7). These cells had an input resistance of 414 ± 205 M Ω . Almost all of these cells (7 of 8, recorded from 7 birds) were sponta-

TABLE 2. Comparison of striatal spiny neurons

	Juvenile	Adult	<i>P</i>	PA	LPO	<i>P</i>
Resting potential, mV	-72 ± 12	-67 ± 10	0.32	-70.7 ± 11.6	-66.3 ± 12.0	0.64
Input resistance, M Ω	314 ± 151 †	435 ± 220	0.15	300 ± 129	614 ± 211	0.01*
AP threshold, mV	-29.2 ± 7.8	-28.8 ± 6.1	0.90	-28.1 ± 7.4	-32.7 ± 5.2	0.15
AP amplitude, mV	45.8 ± 11.3	40.4 ± 10.0	0.18	42.5 ± 9.6	43.9 ± 13.4	0.70
AP duration, ms	1.40 ± 0.27	1.28 ± 0.29	0.37	1.25 ± 0.30	1.23 ± 0.19	0.81
AHP peak, mV	-17.5 ± 5.4	-18.6 ± 3.2	0.58	-17.7 ± 4.2	-20.8 ± 2.0	0.21
AHP time to peak, ms	2.73 ± 1.00	2.81 ± 1.10	0.96	2.82 ± 2.30	3.46 ± 0.50	0.04*
Delay to first spike, ms	406 ± 41	374 ± 84	0.48	389 ± 71	393 ± 55	0.81

Comparison of electrophysiological parameters of juvenile (younger than 50 days) SNs to adult (older than 80 days) SNs, and paleostriatum augmentatum (PA) SNs to lobus parolfactorius (LPO) SNs. Values are compared with the two-tailed Mann-Whitney test. Values in this table are means \pm SD. See METHODS for definitions of the various parameters presented here. The *P* value for each comparison is shown to the right of the values compared. † Data from only 9 cells contributed to this measurement. * These comparisons were significant. The number of cells for juvenile, adult, PA, and LPO SNs were 10 cells from 6 birds, 16 cells from 9 birds, 17 cells from 10 birds, and 5 cells from 4 birds, respectively.

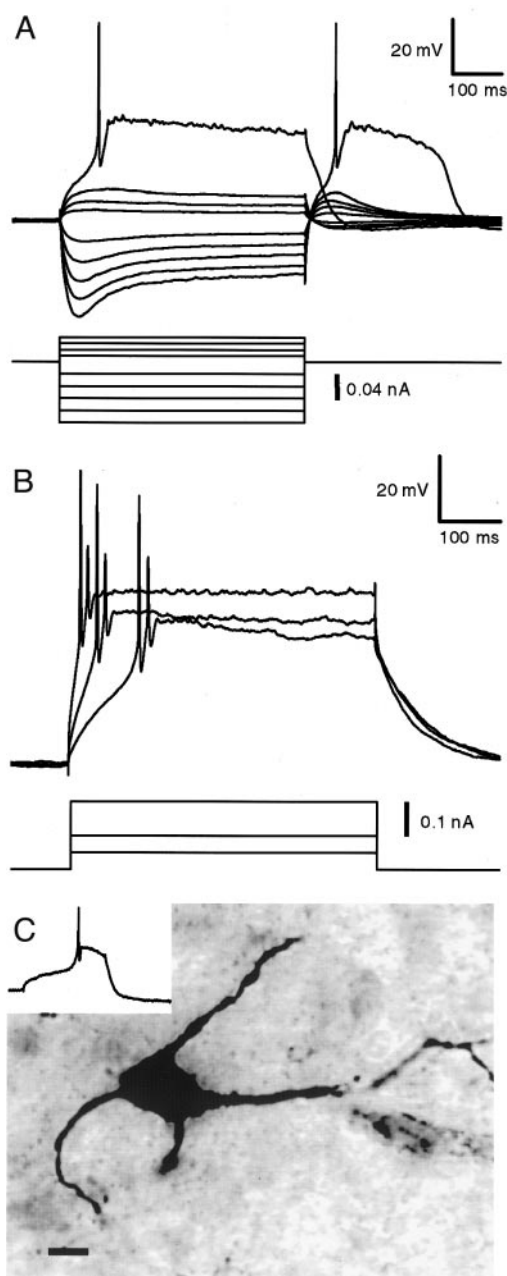


FIG. 5. Intrinsic properties of the low-threshold spike (LTS) cell of avian striatum. *A*: responses of a LTS cell, recorded in LPO, to current pulses delivered from a hyperpolarized potential of -81 mV. This potential was maintained by continuous injection of -0.05 nA current. The largest hyperpolarizing pulse triggered a rebound spike. *B*: responses of a 2nd LTS cell, also in LPO, to suprathreshold current pulses. Note that larger current pulses only triggered the persistent spike more rapidly; they did not evoke more fast spikes. Current pulses were delivered from a baseline potential of -81 mV, maintained by continuous injection of -0.04 nA current. *C*: photomicrograph of a 3rd LTS cell, recorded in PA, filled with neurobiotin. The diameter of this cell is 20 μm along its major axis, larger than any of the SNs or ASNs we filled. *Inset*: a persistent spike evoked in this cell by a $+0.03$ nA pulse delivered from a baseline voltage of -83 mV. Scale bar is 10 μm .

neously active, firing action potentials at regular intervals in the absence of any current injected through the recording electrode (Fig. 7C, average rate: 14 ± 5 Hz). This spontaneous activity sometimes ceased during the recording but was always visible prior to break-in, i.e., could be observed extracellularly

while the recording pipette was forming a seal with the cell's membrane. We therefore hypothesize that the spontaneous activity does not result from changes brought about by the whole cell recording but that the cessation of this activity occurring a few minutes after break-in *does* result from such changes. To study the current-voltage relation of these neurons, we silenced their spontaneous activity by continuously injecting hyperpolarizing current, bringing the cells to a baseline potential near -75 mV. From this baseline potential, hyperpolarizing current pulses evoked a sagging response in membrane voltage, indicating the presence of time-dependent inward rectification (Fig. 7A, $n = 7$ of 8). Subthreshold depolarizing current pulses often evoked a depolarizing bump (Fig. 7A), generally of longer duration than those seen in anomalous SNs. Suprathreshold current pulses evoked regular spiking, with a higher spike rate at the onset of the pulse that declined to a constant rate for the remainder of the pulse (Fig. 7B). Firing rate increased roughly linearly with current amplitude, and most of these cells were capable of sustained firing at high rates (>60 Hz for at least 500 ms, 4 of 6 tested; Fig. 7D). We recovered three of these neurons filled with neurobiotin and found that two possessed thin, beaded, aspiny dendrites (Fig. 7E, both in LPO). One filled cell of this type, recorded in PA, possessed thicker dendrites (0.5 – 2 μm diam), but little else can be said about the morphology of this cell because of the poor quality of the fill. We refer to these neurons as the aspiny, fast-firing (AF) cell type.

Although the AF neuron does not closely resemble any cell type identified in mammalian dorsal striatum, it might be a substantially modified version of one of the striatal interneuron types. One such interneuron type is the cholinergic "long-lasting afterhyperpolarization" (LA) cell (Kawaguchi 1993). To help evaluate the possibility that the AF cells are the avian counterpart of striatal cholinergic interneurons, we compared the morphology of our neurobiotin-labeled AF neurons with zebra finch striatal cells immunostained for choline acetyltransferase (ChAT), the enzyme that synthesizes acetylcholine. ChAT immunostaining labels the somata and proximal dendrites of these presumptively cholinergic neurons, so we compared the thickness of their proximal dendrites (~ 2 μm from the soma). Our two "thin dendrite" AF cells have dendritic diameters of 0.2 – 0.6 μm . The dendrites of ChAT-positive cells are clearly thicker, averaging 1.8 μm diam (range: 1 – 3 μm ; SD: 0.4 μm ; $n = 20$ cells from 2 birds). Our "thick dendrite" AF cell recorded in caudal PA was morphologically more similar to ChAT-positive cells, but because there are apparently no ChAT-positive cells in caudal PA (Li and Sakaguchi 1997; Medina and Reiner 1994; Zuschratter and Scheich 1990; personal observations), it is unlikely that this cell was cholinergic.

Comparison of PA and LPO

Karten and Dubbeldam (1973) have stated that PA and LPO are "strikingly different" in cytology and hodological relationships. We wondered whether these anatomical differences were accompanied by physiological differences in their neurons. All avian striatal cell types we identified (SN, LTS, AF) were found in both structures. We compared the physiological properties of their SNs (the only cell type common enough to permit comparison) and found a statistically significant differ-

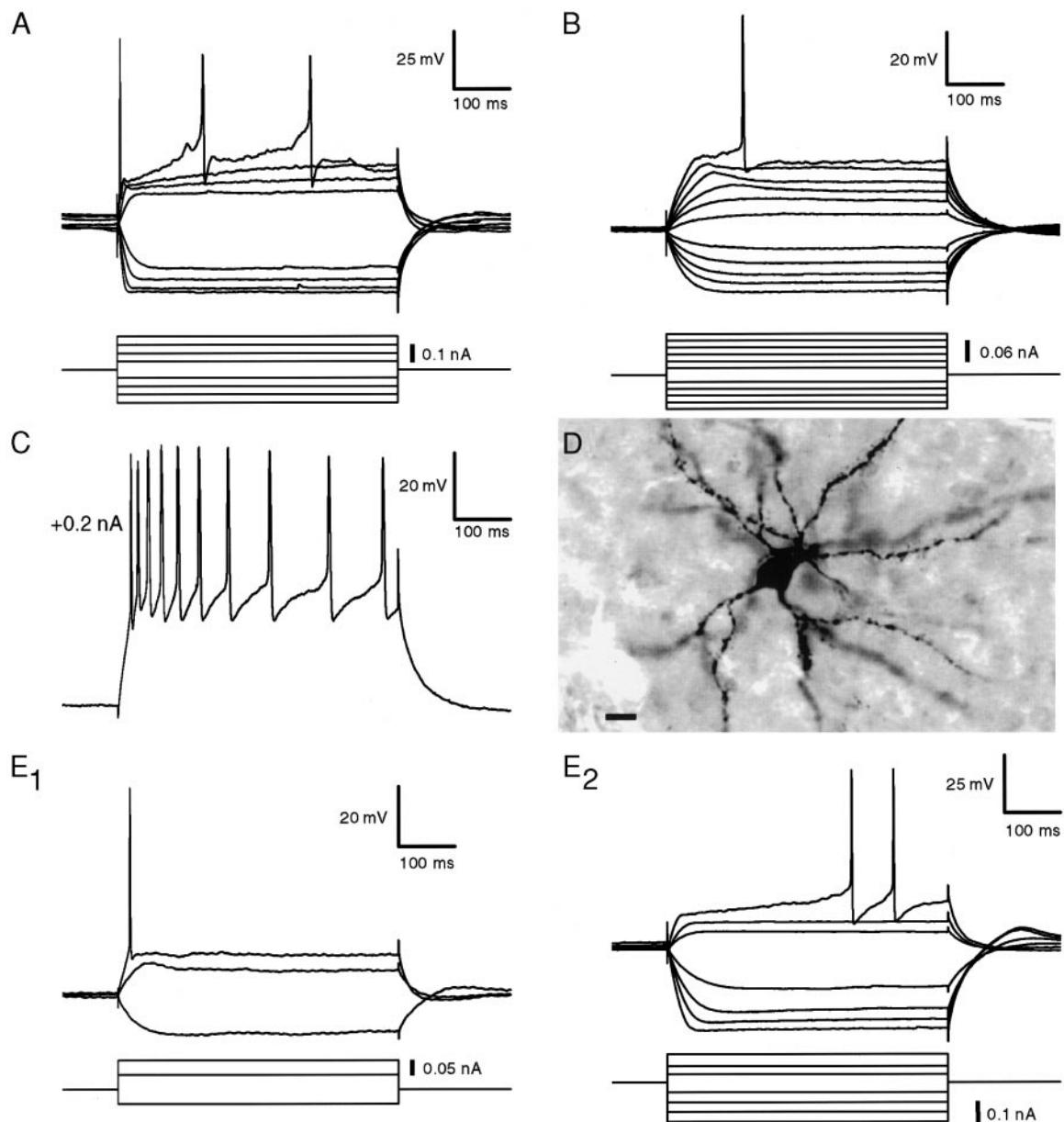


FIG. 6. Intrinsic properties of "anomalous" spiny neurons (ASNs) in avian striatum. *A*: representative ASN showing a ramping response to depolarizing current pulses but lacking delayed spiking. Resting potential was -70 mV. *B*: ASN that seemed to lack the ramping response entirely and instead displayed a small depolarizing "bump" at the onset of depolarizing current pulses. Resting potential was -63 mV. *C*: same cell as in *B*, producing several relatively normal action potentials in response to a $+0.2$ nA current pulse. *D*: photomicrograph of the cell depicted in *B* and *C*, filled with neurobiotin. Scale bar is $10 \mu\text{m}$. *E*: "nonramping" ASN that switched to a normal SN state during the recording. *E1*: response of this cell to current pulses before the switch. *E2*: response of this cell after the switch, showing a ramping response and delayed spiking. Resting potential for this cell was -69 mV. For voltage traces in *A*, *B*, and *E*, the injected current pulses are plotted below the traces. All cells in this figure were recorded in PA.

ence in their input resistance: LPO SNs have higher input resistances ($614 \pm 212 \text{ M}\Omega$, $n = 5$ vs. $300 \pm 129 \text{ M}\Omega$, $n = 16$; Mann-Whitney test, $P = 0.009$), consistent with Karten and Dubbeldam's observation that LPO contains smaller cells on average. The only other statistically significant difference was a longer time to peak for AHPs of LPO SNs (3.46 ± 0.50 vs. 2.82 ± 2.30 ms, $P = 0.04$), which could be due to a longer membrane time constant resulting from the higher input resistance of LPO SNs. A full list of the comparisons made between PA and LPO SNs is shown in Table 2. It is perfectly possible

that there exist physiological differences between the two structures in properties we did not examine, but there were no qualitative physiological differences uncovered by this study.

Intrinsic electrophysiological properties of putative PP neurons

We attempted to record neurons in PP, the avian homologue of the globus pallidus. Obtaining recordings in this region is difficult because the density of cells in PP is low and the

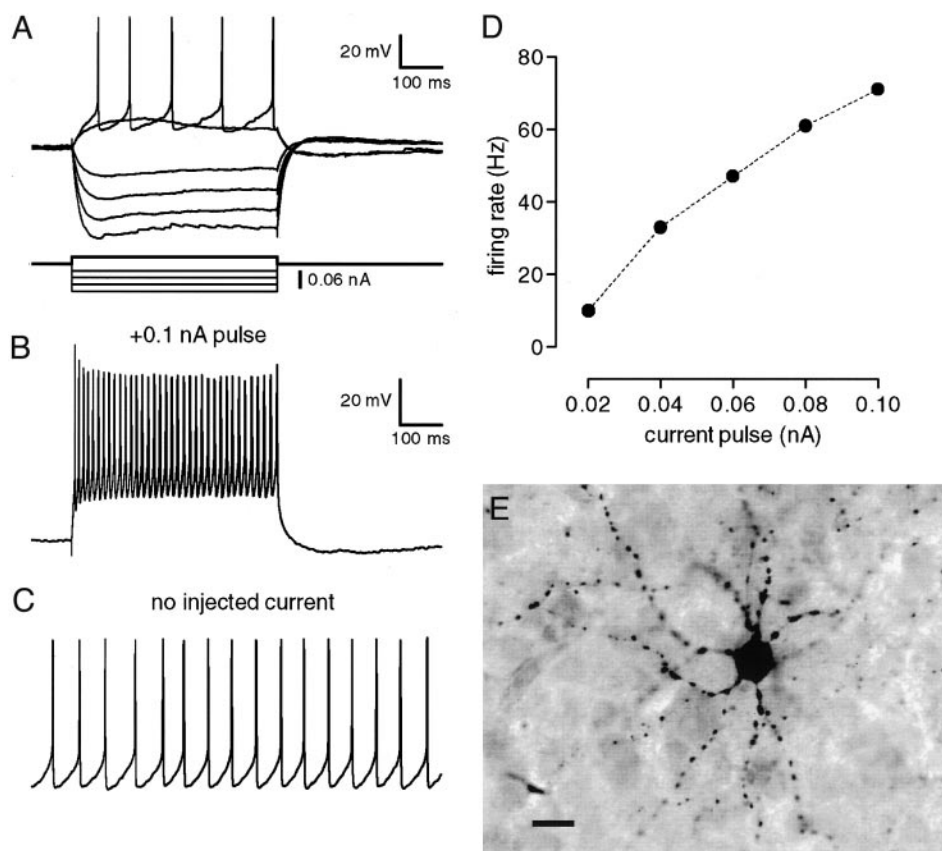


FIG. 7. Intrinsic properties of an aspiny, fast-firing (AF) cell type in avian striatum, recorded in PA. *A*: responses of this cell to a series of 500-ms current pulses. Pulses were delivered from a baseline potential of -78 mV, maintained by continuous injection of -0.03 nA current. The current pulses are plotted immediately below the voltage traces. The 2 depolarizing responses were evoked by distinct current pulses of the *same* magnitude, $+0.02$ nA. This current level is plotted as a thickened line to reflect this fact. *B*: response of this cell to a larger current pulse, illustrating its capacity for firing continuously at a high rate. *C*: spontaneous activity recorded in this neuron; no current was injected through the recording electrode. *D*: action potential frequency evoked in this cell as a function of injected current. Each point represents the average of 2 repetitions of each current pulse; these pulses were delivered from a baseline potential of -78 mV. *E*: photomicrograph of a different AF cell filled with neurobiotin. Scale bar is $10 \mu\text{m}$.

density of fibers is high. Furthermore, PP is a relatively small and narrow region whose borders are not clearly visible in unstained slices (see METHODS). Many of the cells recorded while targeting PP were of the striatal SN type. In all cases where we could confirm the location of such cells using the Nissl stain (5 of 9 SN neurons recorded while targeting PP), they proved to be in PA or on the PA-PP border. Because the Nissl stain degraded the quality of our neurobiotin fills, we could not confirm the locations of all recorded cells in this way. We recorded other cell types while targeting PP that may be representatives of bona-fide PP neurons, but we obtained only a handful of such recordings, and in no case could we be absolutely certain that these cells were in PP. Thus, we offer these “PP recordings” with reservations; some of these neurons may have been in PA.

Two putative PP neurons (recorded from different birds) spontaneously fired bursts of 12–18 action potentials every 5–10 s (Fig. 8A). The membrane potential of these neurons was virtually impossible to control—membrane potential oscillations persisted even when these cells were hyperpolarized by continuous current injection. These cells show some signs of time-dependent inward rectification and tend to fire a burst on rebound following the end of hyperpolarizing current pulses (Fig. 8B). The action potentials of these cells were distinctive in that each spike was usually followed by an afterdepolarization (Fig. 8C); they were the only cells we recorded in the avian basal ganglia that displayed this property. Neither of these bursting cells was recovered after filling with neurobiotin, so their morphology is unknown.

Another group of putative PP cells ($n = 3$ cells from 3 birds) spontaneously fired action potentials at regular inter-

vals (Fig. 9C) and generally resembled the AF cell type of PA and LPO. Like AF neurons, these cells displayed time-dependent inward rectification when hyperpolarized (Fig. 9, A and D). One of these cells displayed a prominent depolarizing bump in membrane potential when injected with a depolarizing current pulse from a hyperpolarized baseline potential (Fig. 9E). Another cell (1 of 2 tested) could sustain firing rates exceeding 60 Hz for at least 500 ms when injected with a strongly depolarizing current pulse (Fig. 9B). One cell was filled with neurobiotin well enough to show the morphology of the dendrites; this cell is shown in Fig. 9F. These three “PP” cells resemble a cell type identified in the rat entopeduncular nucleus (“type I” cells of Nakanishi et al. 1990), the rat homologue of the internal segment of the globus pallidus. This is consistent with the notion that these neurons are avian pallidal cells, but their physiological similarity to the AF cell type of PA and LPO raises doubts concerning their true location.

Unclassified neurons recorded in the paleostriatal complex

We recorded 11 neurons (5 in PA, 3 in LPO, 3 when targeting PP) that we could not classify as a member of any of the cell types described above. Five of these cells bore some resemblance to cholinergic LA or GABAergic “fast-spiking” (FS) interneurons identified in mammalian striatum (3 LA, 2 FS). However, they did not exhibit physiological properties consistent enough to warrant classification into distinct types. The unclassified cells could be singular examples of rare cell types (possibly including types not identified in mammals), damaged examples of the types described above (although

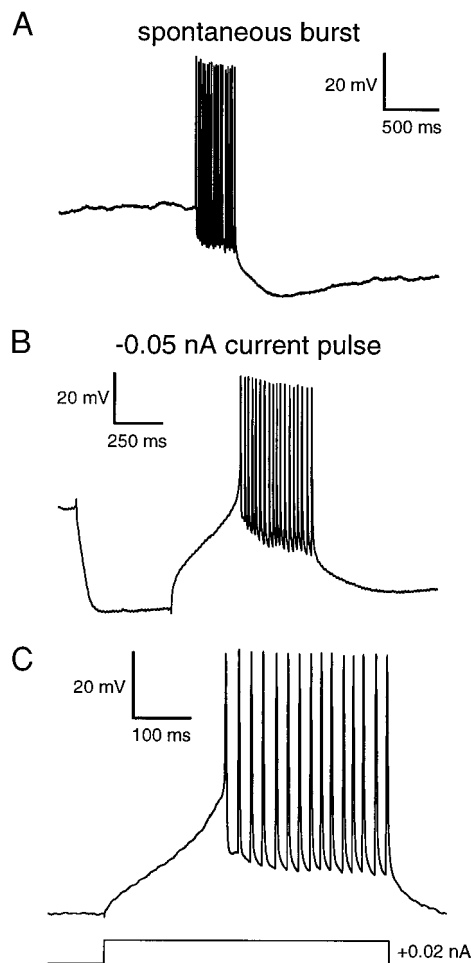


FIG. 8. A spontaneously bursting cell type putatively located in PP. *A*: spontaneous burst of action potentials; no current was injected. *B*: burst triggered on rebound from a 500 ms hyperpolarizing current pulse. Membrane potential at the beginning of traces in *A* and *B* is -50 mV. *C*: magnified view of a burst, illustrating afterdepolarizations that follow the spikes. Burst was triggered by a 500 ms depolarizing current pulse plotted *below* the voltage trace. Membrane potential at the beginning of the trace is -67 mV. *A–C* are from the same cell; we recorded 1 other putative PP neuron exhibiting the same properties.

some of these neurons lacked any overt physiological signs of damage), or cells drawn from a highly variable population of neurons that cannot be divided into distinct types. Further recordings might clarify the nature and significance of these cells.

DISCUSSION

Our main results are that avian striatum contains two cell types that are virtually identical to cell types found in mammalian striatum (SNs and LTS cells). However, avian striatum also contains one cell type (the AF cell) that has not been identified in mammalian striatum. Thus the intrinsic physiological properties of avian striatal neurons are very similar, but *not* identical, to those in mammals.

Similarities between avian and mammalian striatum

The most common cell type we recorded in avian striatum, the spiny neuron, displayed two characteristic physiological

properties that it shared with the principal cell type of mammalian striatum, the medium spiny neuron. First, these cells have fast inward rectification so that their membrane resistance rapidly decreases as they are hyperpolarized. Second, these cells exhibit a ramping response and delayed spiking when depolarized, known to result primarily from the gradual inactivation of an A-type K^+ current in mammals (Nisenbaum and Wilson 1995). Since the ramping response of our SNs shows similar temporal characteristics and is also blocked by 4-AP, an A-type K^+ current probably contributes to the ramp in birds as well. Both the fast inward rectification and the A-type K^+ current can be expected to profoundly influence the response of these neurons to synaptic input (Wilson 1995; Wilson and Kawaguchi 1996).

We also identified one rare class of neuron, the LTS cell, that closely resembles an interneuron type identified in mammalian striatum (Kawaguchi 1993). The defining feature these cells share with their mammalian counterparts is the ability to generate a plateau-like spike that can last for more than 100 ms, generally accompanied by a few conventional fast action potentials near the onset of this persistent spike. The mammalian and avian LTS cells also share a varying degree of time-dependent inward rectification and the tendency to fire on rebound following the end of hyperpolarizing current pulses. We did not observe any qualitative differences between avian and mammalian LTS cells. The LTS cells of mammals contain NADPH diaphorase (Kawaguchi 1993), an enzyme used in the synthesis of nitric oxide. This may also be true of avian LTS cells because avian PA and LPO contain NADPH diaphorase-positive neurons (von Bartheld and Schober 1997; Wallhauser-Franke et al. 1995).

Although we did identify one mammalian striatal interneuron type in avian striatum, the mammalian striatum has two additional physiological classes of interneuron that we did not unambiguously observe in birds: the cholinergic LA neuron and the GABAergic FS neuron (Kawaguchi 1993). However, one cannot conclude that these types are absent in birds; these cells comprise only a tiny fraction of the neurons found in the striatum and thus should be rarely encountered with the blind recording technique we used. Indeed, much of avian striatum (all of LPO, perhaps some of PA) does have a population of presumptively cholinergic neurons containing ChAT (Medina and Reiner 1994; Zuschratter and Scheich 1990). In summary, the data currently available provide no reason to believe that the LA and FS cell types are absent in birds.

Differences between avian and mammalian striatum

We found two prominent differences between avian and mammalian striatum. First, we recorded cells that were morphologically indistinguishable from SNs and yet possessed some physiological properties that have not been recognized in mammalian striatal spiny neurons. We favor the hypothesis that these ASNs are actually SNs that have been damaged or are in an otherwise altered state. In support of this idea, we note that these cells did share some physiological properties with SNs: almost all ASNs displayed fast inward rectification when hyperpolarized and many displayed a ramping response to depolarization. Furthermore, some ASNs exhibited the physiological properties of normal SNs for some time, switching to or from an anomalous state during the recording. ASNs some-

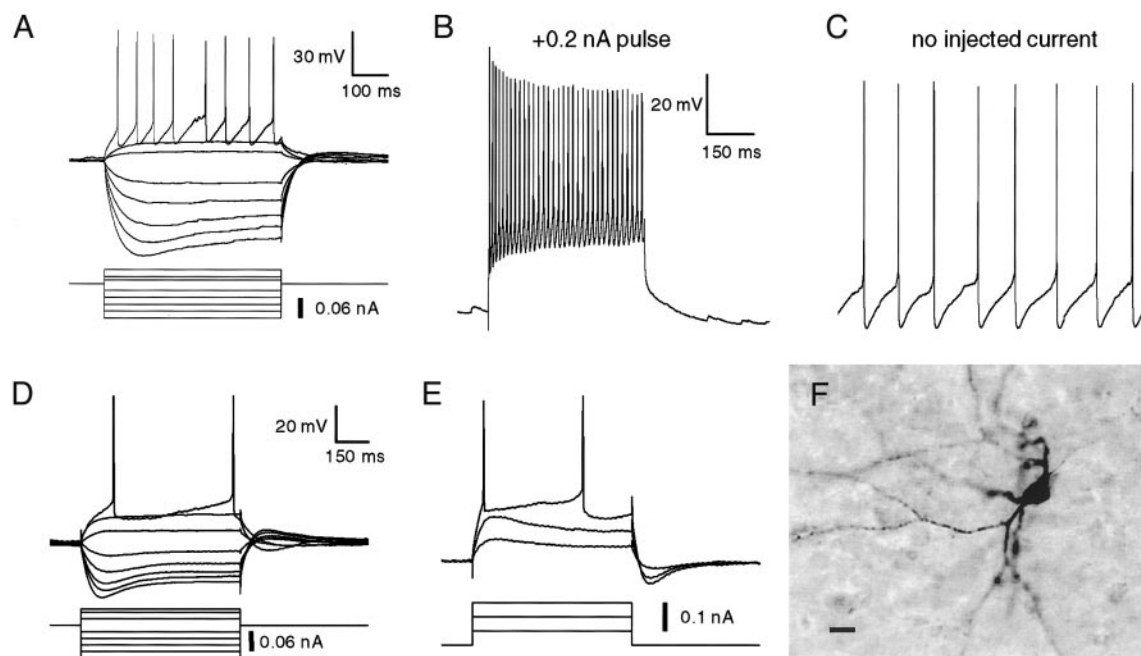


FIG. 9. Intrinsic properties of a fast-firing cell type putatively located in PP. *A*: responses of such a cell to a series of 500 ms current pulses. Pulses were delivered from a baseline potential of -80 mV, maintained by continuous injection of -0.03 nA current. The current pulses are plotted immediately *below* the voltage traces. *B*: response of this cell to a larger current pulse, illustrating its capacity for firing continuously at a high rate. *C*: spontaneous activity recorded in this neuron; no current was injected through the recording electrode. Scale is the same as in *B*. *D*: a 2nd fast-firing cell. This cell was spontaneously active during sealing, but this activity ceased shortly after break-in. Baseline potential is -62 mV. *E*: same cell as in *D*, given current pulses delivered from a hyperpolarized potential (-75 mV) maintained by continuous injection of -0.09 nA. *F*: photomicrograph of the cell depicted in *D* and *E*, filled with neurobiotin. This section was not counterstained with cresyl violet. Scale bar is 10 μ m.

times exhibited other properties associated with unhealthy neurons, such as an inability to fire repetitively or a propensity to fire abnormally small and broad spikes. Finally, there are unpublished observations of ASN-like behavior in mammalian striatum; such behavior is sometimes seen in medium spiny neurons after intracellular dialysis (C. Wilson, personal communication). Nevertheless, it is possible that ASNs represent a population of cells not present in mammalian striatum.

A second difference we discovered between mammalian and avian striatum is the presence of an AF cell type in birds. These cells have no obvious counterpart in mammalian striatum, but we considered the possibility that they are a modified version of the cholinergic LA interneurons or GABAergic FS interneurons of mammals. Mammalian LA neurons are spontaneously active *in vivo* (Wilson et al. 1990) and can be spontaneously active *in vitro* (Bennett and Wilson 1999; but see Kawaguchi 1992 and 1993). In addition, both avian AF cells and mammalian LA cells display time-dependent inward rectification when hyperpolarized (Kawaguchi 1992, 1993). However, avian AF cells fire spontaneously at higher rates than do mammalian LA cells *in vitro* and *in vivo*, and AF cells lack the distinctive long-lasting AHP of LA cells. Most importantly, AF cells appear morphologically distinct from mammalian LA cells *and* ChAT-immunoreactive cells in avian striatum. Thus AF cells are unlikely to be the avian counterpart of cholinergic LA interneurons. AF cells could also be a modified version of the mammalian FS interneuron, but the differences between the two types are substantial: FS cells do not fire spontaneously in slices, do not display time-dependent inward rectification, and

when injected with depolarizing current produce pauses in firing not seen in AF cells (Kawaguchi 1993).

An alternative explanation for the presence of AF cells in avian striatum is that they are functionally globus pallidus (GP) neurons. AF cells closely resemble a cell type recorded in the rat entopeduncular nucleus, the rat homologue of the internal segment of the GP. Specifically, both types are spontaneously active in brain slices, exhibit time-dependent inward rectification, are capable of sustained firing at high rates, and display rebound firing following hyperpolarizing current pulses (Nakanishi et al. 1990). AF cells also resemble a cell type we have tentatively identified in PP, the avian homologue of the GP. Further support for this idea comes from the projections of a specialized region of the LPO found only in songbirds, known as area X. Area X contains the same morphological and physiological cell types we have reported here in PA and LPO, including the AF cell type (Farries and Perkel 1998). Unlike mammalian striatum, but like the mammalian and avian GP, area X projects directly to the thalamus (Nottebohm et al. 1976), and those projection neurons are *not* the spiny neuron type that comprises the projection neurons of mammalian striatum. Instead, the projection neurons of area X are a sparsely distributed population of GABAergic neurons that morphologically resemble the AF cell type (Luo and Perkel 1999). This thalamic projection could be a specialization limited to the song system, but there is evidence that the LPO of nonsinging birds projects to thalamus as well (Székely et al. 1994). The notion that the striatum can harbor "pallidal" cells may seem strange, but it is not unprecedented. The cholinergic

interneurons of mammalian striatum are actually born in the anlage of the GP (the medial ganglionic eminence) and later migrate into the striatum (Olsson et al. 1998). In addition, there are reports that a small subset of the nigral-projecting neurons of mammalian striatum are *not* MSNs, and morphologically resemble neurons of the GP (Bolam et al. 1981; Fisher et al. 1986).

Conclusions

Previous studies have revealed that the mammalian and avian basal ganglia are remarkably similar in their anatomical and neurochemical organization (Medina and Reiner 1995). The present study builds on this work by demonstrating a strong resemblance in the physiological properties of their neurons. Together these results suggest that the basal ganglia of these two vertebrate classes process their inputs in a similar manner, using similar mechanisms. However, we also identified an apparent difference between the basal ganglia of mammals and birds: the presence of the AF cell type in avian striatum.

From the data currently available, the functional significance of this difference is unclear; there are several possibilities. First, the AF cell could represent a new avian striatal cell type or a highly modified version of a cell type found in mammals; this raises the possibility of at least some divergence in basal ganglia function between birds and mammals. Second, the AF cell could be a pallidal cell type that has migrated into avian striatum. This scenario suggests that avian and mammalian basal ganglia might have diverged somewhat in anatomical organization but remain functionally equivalent—the pallidal AF cells might receive input from striatal SNs and project to the standard GP targets (e.g., thalamus), as the example of area X suggests. Third, it is conceivable that the zebra finch striatum is not representative of the striatum of all birds; perhaps only a subset of avian taxa have diverged from an ancestral condition that lacks the AF cell type. Finally, we may be comparing avian PA and LPO to the wrong mammalian structures. Different regions of striatum tend to receive inputs from different regions of pallium e.g., isocortex projects to dorsal striatum and the pallial amygdala projects to ventral striatum (de Olmos and Heimer 1999). There is little doubt that PA and LPO are striatal, but they may not be homologous to mammalian dorsal striatum.

This last possibility is supported by comparisons of mammalian and avian pallium; most of the avian pallium appears to be derived from ventral and lateral pallium (Puelles et al. 1999; Smith-Fernandez et al. 1998; Striedter et al. 1998) and thus would be homologous to the pallial amygdala, piriform cortex, and endopiriform claustrum of mammals (*not* isocortex). If this is true, birds and mammals have undergone expansion of different pallial regions, which may have been accompanied by differential expansion of their associated striatal regions. Thus, the avian striatum may be dominated by homologues of *ventral* striatal regions such as the nucleus accumbens and striatal amygdala, structures that receive input from lateral and ventral pallium. The physiology of these structures has not been as thoroughly studied as that of dorsal striatum; it is conceivable that a mammalian homologue of the AF cell type exists in these regions.

In summary, the results reported here are consistent with the

hypothesis that PA and LPO are homologous to mammalian striatum. However, our results also suggest that it may be premature to conclude that PA and LPO are homologous to *dorsal* striatum; PA and LPO may be more akin to ventral striatum. Parts of the ventral striatum (particularly the extended amygdala) deviate from the canonical pattern of striatal connections and organization (de Olmos and Heimer 1999). It remains to be seen if dorsal and ventral striatum are functionally equivalent, i.e., perform the same kind of processing on different kinds of information. Similarly, we cannot yet say to what degree the avian and mammalian basal ganglia are functionally equivalent, although our data suggest a substantial resemblance. Additional comparative studies measuring cellular physiological properties will be necessary to obtain a full understanding of how basal ganglia function has changed during vertebrate evolution.

We thank L. Stark for the use of ChAT immunostained material from zebra finches. We also thank C. Wilson, D. Jaeger, M. Schmidt, D. Contreras, and J. Cardin for helpful comments during preparation of the manuscript.

REFERENCES

- BENNETT BD AND WILSON CJ. Spontaneous activity of neostriatal cholinergic interneurons in vitro. *J Neurosci* 19: 5586–5596, 1999.
- BLANTON MG, LO TURCO JJ, AND KRIEGSTEIN AR. Whole cell recording from neurons in slices of reptilian and mammalian cerebral cortex. *J Neurosci Methods* 30: 203–210, 1989.
- BOETTIGER CA AND DOUPE AJ. Intrinsic and thalamic excitatory inputs onto songbird LMAN neurons differ in their pharmacological and temporal properties. *J Neurophysiol* 79: 2615–2628, 1998.
- BOLAM JP, SOMOGYI P, TOTTERDELL S, AND SMITH AD. A second type of striatonigral neuron: a comparison between retrogradely labelled and golgi-stained neurons at the light and electron microscopic levels. *Neuroscience* 6: 2141–2157, 1981.
- BOTTJER SW, BRADY JD, AND WALSH JP. Intrinsic and synaptic properties of neurons in the vocal-control nucleus IMAN from in vitro slice preparations of juvenile and adult zebra finches. *J Neurobiol* 37: 642–658, 1998.
- DE OLMOS JS AND HEIMER L. The concepts of the ventral striatopallidal system and extended amygdala. *Ann NY Acad Sci* 877: 1–32, 1999.
- FARRIES MA AND PERKEL DJ. Electrophysiological similarities between area X neurons in the zebra finch and neurons of the mammalian striatum. *Soc Neurosci Abstr* 24: 191, 1998.
- FISHER RS, BUCHWALD NA, HULL CD, AND LEVINE MS. Neurons of origin of striatonigral axons in the cat: connectivity and golgi markers of somatodendritic architecture. *Brain Res* 397: 173–180, 1986.
- JIANG Z-G AND NORTH RA. Membrane properties and synaptic responses of rat striatal neurones in vitro. *J Physiol (Lond)* 443: 533–553, 1991.
- KARTEN HJ. Homology and evolutionary origins of the “neocortex.” *Brain Behav Evol* 38: 264–272, 1991.
- KARTEN HJ AND DUBBELDAM JL. The organization and projections of the paleostriatal complex in the pigeon (*Columba livia*). *J Comp Neurol* 148: 61–90, 1973.
- KAWAGUCHI Y. Large aspiny cells in the matrix of the rat neostriatum in vitro: physiological identification, relation to the compartments and excitatory postsynaptic currents. *J Neurophysiol* 67: 1669–1682, 1992.
- KAWAGUCHI Y. Physiological, morphological, and histochemical characterization of three classes of interneurons in rat neostriatum. *J Neurosci* 13: 4908–5023, 1993.
- KITA T, KITA H, AND KITAI ST. Passive electrical membrane properties of rat neostriatal neurons in an in vitro slice preparation. *Brain Res* 300: 129–139, 1984.
- KITT CA AND BRAUTH SE. A paleostriatal-thalamic-telencephalic path in pigeons. *Neuroscience* 7: 2735–2751, 1982.
- KUENZEL WJ AND MASSON M. *A Stereotaxic Atlas of the Brain of the Chick (Gallus domesticus)*. Baltimore, MD: The Johns Hopkins University Press, 1988.
- LI R AND SAKAGUCHI H. Cholinergic innervation of song control nuclei by the ventral paleostriatum in the zebra finch: a double-labeling study with retrograde fluorescent tracers and choline acetyltransferase immunohistochemistry. *Brain Res* 763: 239–246, 1997.
- LIVINGSTON FS AND MOONEY R. Development of intrinsic and synaptic properties in a forebrain nucleus essential to avian song learning. *J Neurosci* 17: 8997–9009, 1997.

- LUO M AND PERKEL DJ. Long-range GABAergic projection in a circuit essential for vocal learning. *J Comp Neurol* 403: 68–84, 1999.
- MEDINA L AND REINER A. Distribution of choline acetyltransferase immunoreactivity in the pigeon brain. *J Comp Neurol* 342: 497–537, 1994.
- MEDINA L AND REINER A. Neurotransmitter organization and connectivity of the basal ganglia in vertebrates: implications for the evolution of basal ganglia. *Brain Behav Evol* 46: 235–258, 1995.
- MEDINA L AND REINER A. The efferent projections of the dorsal and ventral pallidal parts of the pigeon basal ganglia, studied with biotinylated dextran amine. *Neuroscience* 81: 773–802, 1997.
- NAKANISHI H, KITA H, AND KITAI ST. Intracellular study of rat entopeduncular nucleus neurons in an in vitro slice preparation: electrical membrane properties. *Brain Res* 527: 81–88, 1990.
- NISENBAUM ES AND WILSON CJ. Potassium currents responsible for inward and outward rectification in rat neostriatal spiny projection neurons. *J Neurosci* 15: 4449–4463, 1995.
- NISENBAUM ES, XU ZC, AND WILSON CJ. Contribution of a slowly inactivating potassium current to the transition to firing of neostriatal spiny projection neurons. *J Neurophysiol* 71: 1174–1189, 1994.
- NOTTEBOHM F, STOKES TM, AND LEONARD CM. Central control of song in the canary *Serinus canarius*. *J Comp Neurol* 165: 457–486, 1976.
- OLSSON M, BJÖRKLUND A, AND CAMPBELL K. Early specification of striatal projection neurons and interneuronal subtypes in the lateral and medial ganglionic eminence. *Neuroscience* 84: 867–876, 1998.
- PUELLES L, KUWANA E, PUELLES E, AND RUBENSTEIN JLR. Comparison of the mammalian and avian telencephalon from the perspective of gene expression data. *Eur J Morphol* 37: 139–150, 1999.
- SMITH-FERNANDEZ A, PIEAU C, REPÉRANT J, EDOARDO B, AND WASSEF M. Expression of the *Emx-1* and *Dlx-1* homeobox genes define three molecularly distinct domains in the telencephalon of the mouse, chick, turtle, and frog embryos: implications for the evolution of telencephalic subdivisions in amniotes. *Development* 125: 2099–2111, 1998.
- STARK LL AND PERKEL DJ. Two-stage, input-specific synaptic maturation in a nucleus essential for vocal production in the zebra finch. *J Neurosci* 19: 9107–9116, 1999.
- STRIEDTER GF. The telencephalon of tetrapods in evolution. *Brain Behav Evol* 49: 179–213, 1997.
- STRIEDTER GF, MARCHANT TA, AND BEYDLER S. The “neostriatum” develops as part of the lateral pallium in birds. *J Neurosci* 18: 5839–5849, 1998.
- SZÉKELY AD, BOXER MI, STEWART MG, AND CSILLAG A. Connectivity of the lobus parolfactorius of the domestic chicken (*Gallus domesticus*): an anterograde and retrograde pathway tracing study. *J Comp Neurol* 348: 374–393, 1994.
- VEENMAN CL, WILD JM, AND REINER A. Organization of the avian “cortico-striatal” projection system: a retrograde and anterograde pathway tracing study in pigeons. *J Comp Neurol* 354: 87–126, 1995.
- VON BARTHELD CS AND SCHÖBER A. Nitric oxide synthase in learning-relevant nuclei of the chick brain: morphology, distribution, and relation to transmitter phenotypes. *J Comp Neurol* 383: 135–152, 1997.
- WALLHAUSSER-FRANKE E, COLLINS CE, AND DEVOOGD TJ. Developmental changes in the distribution of NADPH-diaphorase-containing neurons in telencephalic nuclei of the zebra finch song system. *J Comp Neurol* 356: 345–354, 1995.
- WHITE SA, LIVINGSTON FS, AND MOONEY R. Androgens modulate NMDA receptor-mediated EPSCs in the zebra finch song system. *J Neurophysiol* 82: 2221–2234, 1999.
- WILSON CJ. Dynamic modification of dendritic cable properties and synaptic transmission by voltage-gated potassium channels. *J Comp Neurosci* 2: 91–115, 1995.
- WILSON CJ, CHANG HT, AND KITAI ST. Firing patterns and synaptic potentials of identified giant aspiny interneurons in the rat neostriatum. *J Neurosci* 10: 508–519, 1990.
- WILSON CJ AND KAWAGUCHI Y. The origins of two-state spontaneous membrane potential fluctuations of neostriatal spiny neurons. *J Neurosci* 16: 2397–2410, 1996.
- ZUSCHRATTER W AND SCHEICH H. Distribution of choline acetyltransferase and acetylcholinesterase in the vocal motor system of zebra finches. *Brain Res* 513: 193–201, 1990.